# The Nitric Acid−Water Complex: Microwave Spectrum, Structure, and Tunneling

**M. Canagaratna,† J. A. Phillips,‡ M. E. Ott, and K. R. Leopold***

*Department of Chemistry, University of Minnesota, 207 Pleasant Street, SE, Minneapolis, Minnesota 55455*

*Received: October 31, 1997; In Final Form: December 16, 1997*

Eight isotopic derivatives of the complex $HNO_3-H_2O$ have been observed by microwave spectroscopy. The spectra are consistent with a structure in which the nitric acid forms a near-linear, 1.78 Å hydrogen bond to the oxygen of the water. A second, presumably weaker hydrogen bond is formed between a water hydrogen and one of the $HNO_3$ oxygens. The resulting cyclic structure adopts a planar configuration except for the non-hydrogen bonded proton of the $H_2O$. In complexes containing DOH, only the isomer with the deuterium in the plane is observed, confirming the contribution of the secondary O···H interaction to the overall stabilization of the system. Strong evidence for complex internal dynamics involving the water subunit is also presented. The a- and b-type transitions of the $H_2O$ and $D_2O$ containing species exhibit a doubling which disappears in the DOH complex, providing direct evidence for the existence of a proton interchange motion in the system. Moreover, c-type rotational transitions do not appear at their predicted rigid rotor positions, even for the DOH species, providing indirect evidence for a second motion which is interpreted as a large amplitude wagging of the non-hydrogen bonded proton of the water.

## Introduction

Nitric acid plays an important role in the chemistry of the earth's atmosphere. In the troposphere, it is a significant component of acid rain and can react with ammonia to produce ammonium nitrate aerosol.[1,2] In the stratosphere, its hydrates are the primary components of the type I polar stratospheric clouds (PSC's)[3,4] which play a central role in the seasonal depletion of polar ozone.[5,6]

Nitric acid is produced by the three body reaction of $NO_2$ with OH. In the absence of rainout, it is destroyed either by photolysis or by reaction with OH. Its lifetime is long, ranging from days to weeks depending on altitude, making it an important reservoir for $NO_x$ and $HO_x$ species and providing a means by which these two families are coupled.[1] Thus, the balance between the formation and decomposition of $HNO_3$ affects the overall $HO_x$ and $NO_x$ budgets of the atmosphere and, in turn, a wide range of important reactions.

In recent years, there has been a growing interest in the effects of complexation on the chemistry and photophysics of key atmospheric species. Substantial changes in spectroscopy and photochemistry have been documented, for example, in $O_3-H_2O$[7] and $(O_2)_2$.[8] Thus, in light of the many roles that $HNO_3$ plays in the atmosphere, there has been question as to whether complexation with water can impact its chemical and photolytic behavior as well. Tao et al.[9] have calculated the binding energy of $HNO_3-H_2O$ to be 9.5 kcal/mol and from this have estimated that approximately 1% of the atmospheric nitric acid is complexed with water near the earth's surface. Thus, with sufficiently large changes in absorption cross-sections and/or photolysis yields, significant effects could, in principle, be obtained. We note, however, that a very recent study by Carl et al.[10] has shown that, in the *remote* troposphere, the formation of nitric acid hydrates *is not* important, at least in terms of its influence on the ratio of $HNO_3/NO_x$. Nevertheless, the overall activity of atmospheric $HNO_3$ is sufficiently diverse that a fundamental understanding of its complex with water remains a topic of significant interest.

The study of this system is also of fundamental value as it offers molecular level information about the interaction of a strong acid and a single "solvent" molecule. The crystal structures of the mono- and trihydrates have been reported,[11,12] and Raman spectra of liquid, glassy, and crystalline forms of the $HNO_3/H_2O$ binary system have been obtained.[13] The only studies of the isolated 1:1 complex, however, have been limited to a small handful of theoretical calculations[9,14] and low-temperature matrix isolation studies.[15] Thus, a definitive gas phase investigation has been lacking, and in this paper we report the microwave spectrum of the 1:1 binary complex $HNO_3-H_2O$.

## Experimental Section

Rotational spectra were obtained using a pulsed-nozzle Fourier transform microwave spectrometer,[16] the details of which have been given elsewhere.[17] $HNO_3-H_2O$ was initially generated in the gas phase by employing the liquid "drip source" which we previously utilized in our study of $H_2O-SO_3$.[18] Briefly, a hypodermic needle (0.004 in. i.d.; 0.08 in. o.d.) was connected to a small reservoir of liquid water and inserted a few millimeters downstream of the nozzle orifice, thus allowing liquid to evaporate directly into the supersonic expansion. In this work, argon was passed over a 90% solution of $HNO_3$ and expanded through a 0.8 mm nozzle at a stagnation pressure of 1.7 atm.

The experiments involving deuterium substitution revealed an interesting feature of this source which eventually led us to modify our method of production of the complex. In particular, during attempts to make the mixed H/D isotopic species, we observed extensive isotopic scrambling between the nitric acid and the water. For example, injection of $D_2O$ into an $Ar/HNO_3$

* Corresponding author.
† Present address: Massachusetts Institute of Technology, 77 Massachusetts Ave., Building 54, Room 1320, Cambridge, MA 02139.
‡ Present address: Department of Chemistry and Biochemistry, University of Colorado, Boulder, CO 80309.

S1089-5639(98)00033-4 CCC: $15.00 
Published on Web 02/06/1998

expansion resulted in the formation not only of the desired $HNO_3-D_2O$ complex but also of a variety of other deuterated species such as $DNO_3-H_2O$ and $HNO_3-DOH$ as well. Similar results were obtained by evaporating $H_2O$ into an $Ar/DNO_3$ expansion. Thus, while the drip source was very effective at producing the parent complex, it suffered a serious loss in selectivity in forming partially deuterated derivatives. The resulting spectral congestion and consequent isotopic signal dilution turned out to be unacceptable, especially while searching for the rather weak b-type transitions, and thus an alternate method of production was sought.

The most successful method employed a large bore needle (0.012 in. i.d.; 0.22 in. o.d.) with the usual 90° bend to "co-inject"[19] pure water *vapor* at its ambient vapor pressure into the pulse of argon and nitric acid. With use of this arrangement, transition intensities for the parent species were both extremely stable and comparable in intensity to those obtained with the liquid water drip source. However, little if any isotopic scrambling was observed in experiments involving deuterium substitution, suggesting that the H/D exchange in the drip source takes place on exposed surfaces of bulk liquid as it evaporates into the vacuum chamber.

Rotational transitions of $HNO_3-H_2O$ were first identified by their characteristic $^{14}N$ quadrupole hyperfine structure and by their dependence on $H_2O$. Subsequent confirmation was achieved by the ability to predict and observe additional transitions for both the parent complex and its isotopomers. The $^{15}N$ containing species was observed in natural abundance, but isotopically enriched samples were used to obtain the spectra of the deuterated and $^{18}O$ substituted derivatives.

The $DNO_3$ used in these experiments was synthesized "in house" from $NaNO_3$ and $D_2SO_4$.[20] Approximately 26.85 g of $NaNO_3$ and 50.0 g of $D_2SO_4$ (98% D enriched) were mixed together, and the resulting $DNO_3$ was vacuum distilled (under aspirator vacuum) at a temperature of approximately 75 °C into a cooled receiving flask. A slight excess of $D_2SO_4$ was maintained in the reaction mixture to ensure that the collected $DNO_3$ would be dry. Typically, anywhere from 4 to 6 mL of $DNO_3$ was collected from this synthesis.

## Results

The microwave spectra of $HNO_3-H_2O$, $H^{15}NO_3-H_2O$, $HNO_3-H_2{}^{18}O$, $HNO_3-D_2O$, $HNO_3-DOH$, $DNO_3-H_2O$, $DNO_3-D_2O$, and $DNO_3-DOH$ were obtained in this study. For both of the DOH species observed, the spectra correspond to the form with the deuterium in the hydrogen bond and the proton free (see the section below on "Structure Determination"). No evidence was found for the hydrogen bonded isomer.

The a-type spectra were recorded for all of the isotopomers examined, and the significantly weaker b-type transitions were measured for all but the $H^{15}NO_3-H_2O$ and $DNO_3-DOH$ species. Hyperfine-free line centers were determined as described in the next section and are listed in Tables 1 and 2. A complete tabulation of spectral data (including individual hyperfine frequencies) is rather extensive and may be obtained either from the authors or as Supporting Information.

The existence of two tunneling states, designated in this work by A and B, was readily apparent from the spectra of $HNO_3-H_2O$, $HNO_3-H_2{}^{18}O$, $DNO_3-H_2O$, $HNO_3-D_2O$, and $DNO_3-D_2O$. The b-type transitions of these species were all doubled, with splittings of ~5 MHz for the $H_2O$ containing complexes and ~0.8 MHz for the $D_2O$ containing derivatives.[21] The two sets of spectra were distinguishable according to their intensity (see below), with A and B state transitions occurring in a ratio of approximately 1:3 for complexes containing $H_2O$ and 2:1 for the species containing $D_2O$.[22]

For $HNO_3-DOH$, however, careful searches about the measured b-type transitions failed to reveal evidence of another state. A search of ±20 MHz, for example, was performed around the observed $3_{03}-3_{12}$ transition, while a similar search of +10 and −20 MHz was conducted around the $2_{02}-2_{11}$ transition. Given the intensity with which these lines were observed, and considering the ≤5 MHz window in which their tunneling partners occurred for the $H_2O$ and $D_2O$ containing species, a second set of spectra, had it existed, should have been observed under the search conditions used.

While the spectral doubling in the $H_2O$ and $D_2O$ containing species was most obvious in the b-type transitions, the a-type spectra also exhibited evidence of tunneling. In the case of $H^{15}NO_3-H_2O$, for which the spectra were free of hyperfine structure, two sets of a-type transitions were clearly observed. The splittings were small, however, and thus for the other isotopic forms of the complex, the tunneling doublings were highly convoluted with $^{14}N$ (and in some cases deuterium) hyperfine structure. Nevertheless, after careful analysis, two distinct sets of a-type spectra were identified for $HNO_3-H_2O$ and $HNO_3-H_2{}^{18}O$. In the a-type transitions of $DNO_3-H_2O$ and the $D_2O$ containing derivatives, however, the dense and only partially resolved hyperfine structure precluded a similar analysis. Again, as for the b-type transitions, no evidence of tunneling was observed in the a-type spectra of the DOH containing species.

The structure of the complex as determined by ab initio calculation[9] contains an out-of-plane OH bond oriented so as to produce a dipole moment component of approximately 0.7 D along the *c*-axis of the complex. Thus, in principle, c-type transitions should be allowed for these systems. For the $H_2O$ containing adducts, however, careful searches in a ±10 MHz window around the predicted $3_{03}-3_{13}$ and $2_{02}-2_{12}$ transitions failed to reveal any evidence of molecular absorptions. Similarly, for the $D_2O$ and DOH containing species, no c-type transitions were obtained in the ±5 MHz region around their predicted frequencies. Since all of the a-type and b-type spectra were observed within a few hundred kilohertz of their rigid rotor predictions, these observations suggest that there are no rigid rotor c-type transitions in these complexes.

**Spectral Analysis.** The analysis of the spectra was divided into two parts. First, since most of the transitions were split due to hyperfine structure, hyperfine-free line centers were obtained for each observed transition. For $HNO_3-H_2O$ and $HNO_3-H_2{}^{18}O$, where the hyperfine structure was well-resolved in most rotational transitions observed, a least squares fit using the usual first order treatment for a single coupling nucleus[23] was employed to obtain quadrupole coupling constants and line centers. For $DNO_3-H_2O$ and $HNO_3-DOH$, the hyperfine structure was only partially resolved in most of the observed spectra, but, in several transitions of these species, a detailed hyperfine analysis was possible as well. Again, the usual first order approach was used, this time for two coupling nuclei.[23,24] In all cases, the fitted hyperfine frequencies were commensurate with the experimental uncertainties. The line centers obtained are given in Tables 1 and 2 (see also Figure 1), and the quoted uncertainties are two standard errors in the fits. The hyperfine constants are given in Table 3.

In the remaining isotopic derivatives, where multiple quadrupolar nuclei precluded adequate resolution of the hyperfine structure, a weighted average of the observed peaks was used

**TABLE 1: Hyperfine-Free Line Centers of $H_2O$ and $D_2O$ Containing Isotopomers of the Nitric Acid−Water Complex**

| transition | state A (MHz) | (obs − calc)[a] (kHz) | state B (MHz) | (obs − calc)[a] (kHz) |
|---|---|---|---|---|
| | | $HNO_3-H_2O$ | | |
| $0_{00}-1_{01}$ | 4 901.845(6)[b] | 12 | 4 901.845(6)[b] | 4 |
| $1_{01}-2_{02}$ | 9 786.183(4)[b] | −9 | 9 786.213(4)[b] | 1 |
| $1_{11}-2_{12}$ | 9 324.875(5)[b] | 5 | 9 325.020(5)[b] | −3 |
| $1_{10}-2_{11}$ | 10 282.301(4)[b] | 10 | 10 282.174(5)[b] | 2 |
| $2_{02}-3_{03}$ | 14 635.756(5)[b] | 1 | 14 635.795(6)[b] | 0 |
| $2_{12}-3_{13}$ | 13 976.478(12)[e] | 6 | 13 976.710(12)[e] | 1 |
| $2_{11}-3_{12}$ | 15 412.185(20)[e] | −22 | 15 411.944(20)[e] | −41 |
| $2_{21}-3_{22}$ | 14 705.095(4)[b] | −2 | 14 705.128(4)[b] | 7 |
| $2_{20}-3_{21}$ | *d* | | 14 774.631(4)[b] | −8 |
| $0_{00}-1_{11}$ | *d* | | 14 520.416(6)[b] | −7 |
| $1_{01}-1_{10}$ | 10 101.983(5)[b] | 2 | 10 097.156(5)[b] | 0 |
| $2_{02}-2_{11}$ | 10 598.084(5)[b] | 4 | 10 593.126(4)[b] | 10 |
| $3_{03}-3_{12}$ | 11 374.529(4)[b] | −3 | 11 369.347(4)[b] | −8 |
| | | $HNO_3-H_2{}^{18}O$ | | |
| $0_{00}-1_{01}$ | 4 630.238(6)[b] | −1 | 4 630.261(6)[b] | −4 |
| $1_{01}-2_{02}$ | 9 246.706(5)[b] | −5 | 9 246.757(5)[b] | −11 |
| $1_{11}-2_{12}$ | 8 832.821(4)[b] | 1 | 8 832.991(5)[b] | −4 |
| $1_{10}-2_{11}$ | 9 687.965(4)[b] | 1 | 9 687.897(6)[b] | −3 |
| $2_{02}-3_{03}$ | 13 835.742(6)[b] | −3 | 13 835.823(5)[b] | −16 |
| $2_{12}-3_{13}$ | 13 240.670(24)[e] | 15 | 13 240.935(24)[e] | 10 |
| $2_{11}-3_{12}$ | 14 523.077(22)[e] | −19 | 14 522.973(22)[e] | −35 |
| $2_{21}-3_{22}$ | *d* | | 13 890.417(4)[b] | 9 |
| $2_{20}-3_{21}$ | 13 945.071(6)[b] | 8 | 13 945.150(6)[b] | −1 |
| $1_{01}-1_{10}$ | 10 211.019(5)[b] | −1 | 10 206.257(5)[b] | 0 |
| $2_{02}-2_{11}$ | 10 652.278(8)[b] | 5 | 10 647.391(5)[b] | 1 |
| $3_{03}-3_{12}$ | *d* | | 11 334.537(16) | −21 |
| | | $H^{15}NO_3-H_2O$ | | |
| $0_{00}-1_{01}$ | 4 887.218(10)[c] | 10 | 4 887.218(8)[c] | 4 |
| $1_{01}-2_{02}$ | 9 757.147(8) | −13 | 9 757.181(8) | 3 |
| $1_{11}-2_{12}$ | 9 298.445(8) | 0 | 9 298.595(8) | −2 |
| $1_{10}-2_{11}$ | 10 250.242(8) | 0 | 10 250.116(8) | −2 |
| $2_{02}-3_{03}$ | 14 592.758(10) | 7 | 14 592.790(10) | −1 |
| | | $DNO_3-H_2O$ | | |
| $0_{00}-1_{01}$ | 4 873.132[b] | −1 | 4 873.132[b] | −1 |
| $1_{01}-2_{02}$ | 9 728.500(80)[c,e] | −5 | 9 728.500(80)[c,e] | 1 |
| $1_{11}-2_{12}$ | 9 267.144(66)[c,e] | 74 | 9 267.144(66)[c,e] | 25 |
| $1_{10}-2_{11}$ | 10 225.272(64)[c,e] | −10 | 10 225.272(64)[c,e] | 38 |
| $2_{02}-3_{03}$ | 14 548.501(48)[c,e] | −19 | 14 548.501(48)[c,e] | 6 |
| $2_{11}-3_{12}$ | 15 326.405(52)[c,e] | −99 | 15 326.405(52)[c,e] | −20 |
| $2_{12}-3_{13}$ | 13 889.674(52)[c,e] | 78 | 13 889.674(52)[c,e] | 11 |
| $2_{21}-3_{22}$ | 14 619.038(54)[c,e] | 53 | 14 619.038(54)[c,e] | 56 |
| $2_{20}-3_{21}$ | 14 689.726(42)[c,e] | 95 | 14 689.726(42)[c,e] | 75 |
| $1_{01}-1_{10}$ | *d* | | 9 955.554(40)[e] | −4 |
| $2_{02}-2_{11}$ | 10 457.345(32)[e] | −64 | 10 452.297(44)[e] | 5 |
| $3_{03}-3_{12}$ | 11 235.465(34)[e] | 71 | 11 230.211(40)[e] | −12 |
| | | $HNO_3-D_2O$ | | |
| $0_{00}-1_{01}$ | 4 570.097(34)[c,e] | −8 | 4 570.097(34)[c,e] | 0 |
| $1_{01}-2_{02}$ | 9 126.401(42)[c,e] | 10 | 9 126.401(42)[c,e] | 20 |
| $1_{11}-2_{12}$ | 8 717.926(60)[c,e] | −17 | 8 717.926(60)[c,e] | −11 |
| $1_{10}-2_{11}$ | 9 562.315(56)[c,e] | −3 | 9 562.315(56)[c,e] | 10 |
| $2_{02}-3_{03}$ | 13 655.112(44)[c,e] | −26 | 13 655.112(44)[c,e] | −23 |
| $2_{11}-3_{12}$ | 14 334.554(44)[c,e] | −49 | 14 334.554(44)[c,e] | −44 |
| $2_{12}-3_{13}$ | 13 068.327(32)[c,e] | 4 | 13 068.327(32)[c,e] | 0 |
| $2_{21}-3_{22}$ | 13 709.986(44)[c,e] | 49 | 13 709.986(44)[c,e] | 49 |
| $2_{20}-3_{21}$ | 13 764.947(50)[c,e] | 29 | 13 764.947(50)[c,e] | 26 |
| $1_{01}-1_{10}$ | 9 916.159(48)[e] | −33 | 9 915.430(48)[e] | −17 |
| $2_{02}-2_{11}$ | 10 352.117(52)[e] | −2 | 10 351.375(46)[e] | 5 |
| $3_{03}-3_{12}$ | 11 031.607(40)[e] | 23 | 11 030.839(32)[e] | 5 |
| | | $DNO_3-D_2O$ | | |
| $0_{00}-1_{01}$ | 4 547.019(60)[c,e] | 13 | 4 547.019(60)[c,e] | 21 |
| $1_{01}-2_{02}$ | 9 079.847(64)[c,e] | −40 | 9 079.847(64)[c,e] | −32 |
| $1_{11}-2_{12}$ | 8 670.278(54)[c,e] | −52 | 8 670.278(54)[c,e] | −50 |
| $1_{10}-2_{11}$ | 9 517.524(68)[c,e] | −9 | 9 517.524(68)[c,e] | 5 |
| $2_{02}-3_{03}$ | 13 584.581(54)[c,e] | −40 | 13 584.581(54)[c,e] | −47 |
| $2_{11}-3_{12}$ | 14 267.189(46)[c,e] | −37 | 14 267.189(46)[c,e] | −37 |
| $2_{12}-3_{13}$ | 12 996.710(46)[c,e] | −4 | 12 996.710(46)[c,e] | −22 |
| $2_{21}-3_{22}$ | 13 640.741(54)[c,e] | 106 | 13 640.741(54)[c,e] | 97 |
| $2_{20}-3_{21}$ | 13 696.919(60)[c,e] | 89 | 13 696.919(60)[c,e] | 76 |
| $1_{01}-1_{10}$ | *d* | | 9 769.342(40)[e] | 4 |
| $2_{02}-2_{11}$ | 10 207.766(40)[e] | 3 | 10 206.988(28)[e] | 9 |
| $3_{03}-3_{12}$ | *d* | | 10 899.568(22)[e] | −9 |

[a] Residuals from fit to eq 1. [b] Line centers from fit to hyperfine structure. Uncertainties are 2 standard errors in the fit. [c] Tunneling doubling not resolved. The same frequency is assumed for both states. [d] Not observed. [e] Line centers obtained from a weighted average of partially resolved hyperfine components. Numbers in parentheses are the estimated uncertainties. See text for details.

**TABLE 2: Hyperfine-Free Line Centers of $HNO_3$−DOH and $DNO_3$−DOH[a]**

| transition | freq (MHz) | (obs − calc)[b] (kHz) |
|---|---|---|
| | $HNO_3$−DOH | |
| $0_{00}-1_{01}$ | 4 792.125(3)[c] | 2 |
| $1_{01}-2_{02}$ | 9 567.332(60)[d] | −7 |
| $1_{11}-2_{12}$ | 9 117.950(3)[c] | −2 |
| $1_{10}-2_{11}$ | 10 050.364(2)[c] | −1 |
| $2_{02}-3_{03}$ | 14 308.863(74)[d] | −20 |
| $2_{12}-3_{13}$ | 13 666.459(94)[d] | 24 |
| $2_{11}-3_{12}$ | 15 064.642(74)[d] | −32 |
| $2_{21}-3_{22}$ | 14 376.012(30)[d] | 56 |
| $2_{20}-3_{21}$ | 14 443.206(32)[d] | −6 |
| $1_{01}-1_{10}$ | 9 903.034(60)[d] | 7 |
| $2_{02}-2_{11}$ | 10 386.055(56)[d] | 1 |
| $3_{03}-3_{12}$ | 11 141.852(62)[d] | 7 |
| | $DNO_3$−DOH | |
| $0_{00}-1_{01}$ | 4 765.424(27)[d] | −42 |
| $1_{01}-2_{02}$ | 9 513.659(32)[d] | −10 |
| $1_{11}-2_{12}$ | 9 063.534(40)[d] | 6 |
| $1_{10}-2_{11}$ | 9 998.193(62)[d] | 15 |
| $2_{02}-3_{03}$ | 14 227.499(26)[d] | −1 |
| $2_{11}-3_{12}$ | 14 986.180(60)[d] | 0 |
| $2_{21}-3_{22}$ | 14 296.068(44)[d] | 47 |
| $2_{20}-3_{21}$ | 14 364.717(48)[d] | −7 |

[a] Both species correspond to the isomer with the deuterium of the water in the plane. [b] Residuals from fit to eq 1. [c] Line center from fit to hyperfine structure. Uncertainties are 2 standard errors in the fit. [d] Line centers obtained from a weighted average of partially resolved hyperfine components. Numbers in parentheses are the estimated uncertainties. See text for details.

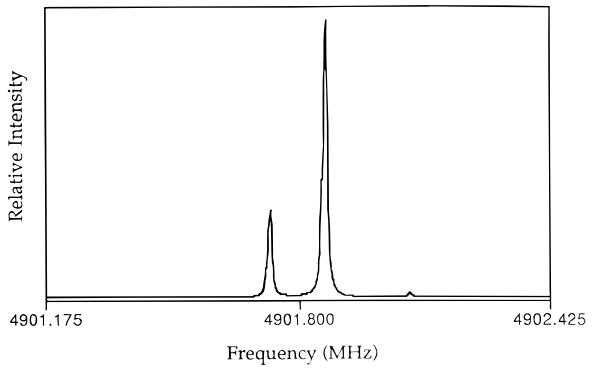


**Figure 1.** The three nuclear quadrupole hyperfine components in the $J = 1 \leftarrow 0$ transition of $HNO_3$−$H_2O$. This spectrum represents a total data collection time of 127 s.

to obtain and estimate of the hypothetical line centers. The uncertainty in the weighted average was explicitly calculated by taking into account the uncertainties in each of the partially resolved components. However, since this average often included unresolved components from both states of the complex, and since the intensities of the components themselves varied depending on the cavity frequency, a conservative estimate of the overall uncertainty in the line centers was obtained by doubling the calculated error in the weighted average. Thus, depending on the transition, the estimated uncertainties obtained in this way range from approximately 20 to 100 kHz. These results are also presented in Tables 1 and 2. For transitions with unresolved tunneling doubling, a common line center was assigned to both the A and B states of the complex.

In the second part of the analysis, the hyperfine-free line centers of each of the isotopomers were fit to Watson's Hamiltonian for a distortable asymmetric rotor,[25] viz.,

$$H = [(B + C)/2 - \Delta_J \mathbf{J}^2]\mathbf{J}^2 + [A - (B + C)/2 - \Delta_{JK}\mathbf{J}^2 - \Delta_K \mathbf{J}_z^2]\mathbf{J}_z^2 + [(B - C)/2 - 2\delta_J \mathbf{J}^2](\mathbf{J}_x^2 - \mathbf{J}_y^2) - \delta_K[\mathbf{J}_z^2(\mathbf{J}_x^2 - \mathbf{J}_y^2) + (\mathbf{J}_x^2 - \mathbf{J}_y^2)\mathbf{J}_z^2] \quad (1)$$

where $A$, $B$, and $C$ are the rotational constants and $\Delta_J$, $\Delta_{JK}$, $\Delta_K$, $\delta_J$, and $\delta_K$ are centrifugal distortion constants. When two states were observed for a given isotopomer, separate spectral fits were done for each. For $HNO_3$−$H_2O$ and $HNO_3$−$H_2{}^{18}O$, where the hyperfine structure was resolved in most of the transitions observed, the line centers were readily fit to $[A - (B + C)/2]$, $(B - C)/2$, $(B + C)/2$, $\Delta_J$, and $\Delta_{JK}$.[26] For species with mostly unresolved hyperfine structure, however, the averaged rotational line centers were not determined with enough accuracy to justify fitting the $\Delta_{JK}$ term. Thus, for these species, the fits were performed by fixing $\Delta_{JK}$ at the value obtained for the A state of the $HNO_3$−$H_2O$ complex. From the second term in the Hamiltonian, it can be seen that A is not well-determined if the transitions that change $K_{-1}$ are not measured. Therefore, in $H^{15}NO_3$−$H_2O$ and $DNO_3$−DOH, whose b-type transitions were not measured, the value of $A$ is somewhat poorly determined. The residuals from the fit are listed in Tables 1 and 2, and the spectroscopic constants are summarized in Table 4.

**Tunneling.** The observation of two states in the spectra of the $H_2O$ and $D_2O$ containing isotopomers is indicative of internal motions within the complex. Moreover, the mass-dependent reduction in the tunneling doubling from ∼5.0 MHz in the b-type transitions of the $H_2O$ containing species to ∼0.8 MHz in those in the $D_2O$ derivatives is consistent with a motion involving the hydrogen atoms of the water subunit. The disappearance of the doubling in $HNO_3$−DOH indicates that the motion involves an interchange of the H or D atoms on the water.

The observed intensities of the A and B state transitions support this conclusion. For $H_2O$ containing species, Fermi−Dirac statistics require that the total wave function of the complex be antisymmetric with respect to H atom interchange. Thus, the symmetric ($I = 1$) and antisymmetric ($I = 0$) spin functions which arise from the two $I = {}^1/_2$ hydrogen nuclei can only be paired with the spatially symmetric (A) and antisymmetric (B) tunneling states, respectively. Since the $I = 1$ spin wave function has a statistical weight of 3 and the $I = 0$ spin wave function has a statistical weight of 1, an intensity ratio of 1:3 is expected for the A and B state transitions, in agreement with experiment. Similarly, for species which contain $D_2O$, Bose−Einstein statistics dictate that the total wave function must be symmetric with respect to exchange of the two $I = 1$ deuterium nuclei. This results in the combination of the symmetric A state with the symmetric spin functions ($I = 0, 2$) of statistical weight 6, and the antisymmetric B state with the antisymmetric spin function ($I = 1$) of statistical weight 3. Thus, in this case, the A and B state transitions occur in a 6:3 intensity ratio, also in agreement with experimental observation.

The absence of c-type transitions at the frequencies predicted by a rigid rotor Hamiltonian contains further information about the internal dynamics of the complex. Since the transitions allowed by $\mu_a$ and $\mu_b$ occur at their rigid rotor frequencies, we surmise that the a- and b-type transitions of the complex occur *within* a particular tunneling state and therefore that these components of the dipole moment are symmetric with respect to the tunneling motion. On the other hand, the *absence* of rigid rotor c-type transitions can be interpreted in two ways. One possibility, of course, is that $\mu_c$ is zero. The other is that $\mu_c$ is not zero but is inverted by the tunneling motion, thus

**TABLE 3: Observed Quadrupole Coupling Constants of $HNO_3-H_2O$ and Its Isotopomers[a]**

| species (state) | $eQq_{aa}$(N) (MHz) | $[eQq_{bb} - eQq_{cc}]$(N) (MHz) | $eQq_{aa}$(D) (MHz) | $[eQq_{bb} - eQq_{cc}]$(D) (MHz) |
|---|---|---|---|---|
| $HNO_3-H_2O$ (A) | −0.4682(34) | 0.3184(83) | | |
| $HNO_3-H_2O$ (B) | −0.4670(31) | 0.3090(76) | | |
| $HNO_3-H_2{}^{18}O$ (A) | −0.4688(40) | 0.3044(94) | | |
| $HNO_3-H_2{}^{18}O$ (B) | −0.4722(34) | 0.300(11) | | |
| $DNO_3-H_2O$ (A, B) | −0.462(10) | *b* | 0.161(13) | *c* |
| $HNO_3$−DOH | −0.4859(76) | 0.2947(88) | 0.1182(52) | −0.4285(77) |

[a] Uncertainties are 1 standard error in the fits. [b] Fixed at 0.3 MHz because $[eQq_{bb} - eQq_{cc}]$ cannot be determined from the $0_{00}-1_{01}$ transition. [c] Fixed at 0.0 MHz because $[eQq_{bb} - eQq_{cc}]$ cannot be determined from the $0_{00}-1_{01}$ transition.

**TABLE 4: Rotational and Distortion Constants of $HNO_3-H_2O$ and Its Isotopomers[a]**

| species (state) | *A* (MHz) | *B* (MHz) | *C*(MHz) | $\Delta_J$ (kHz) | $\Delta_{JK}$ (kHz) |
|---|---|---|---|---|---|
| $HNO_3-H_2O$ (A) | 12 313.5626(28) | 2690.2762(9) | 2211.5660(9) | 2.295(26) | 7.572(63) |
| $HNO_3-H_2O$ (B) | 12 308.8097(18) | 2690.2119(8) | 2211.6378(8) | 2.192(5) | 7.961(38) |
| $HNO_3-H_2{}^{18}O$ (A) | 12 312.3731(28) | 2528.9100(8) | 2101.3380(8) | 2.318(13) | 7.46(14) |
| $HNO_3-H_2{}^{18}O$ (B) | 12 307.6823(29) | 2528.8632(10) | 2101.4107(10) | 2.211(5) | 7.30(5) |
| $H^{15}NO_3-H_2O$ (A) | 12 307.1(43) | 2681.5565(43) | 2205.6581(43) | 1.735(65) | *b* |
| $H^{15}NO_3-H_2O$ (B) | 12 303.8(22) | 2681.4908(31) | 2205.7303(31) | 1.700(41) | *b* |
| $DNO_3-H_2O$ (A) | 12 157.665(48) | 2676.1237(84) | 2197.0179(84) | 2.39(12) | *b* |
| $DNO_3-H_2O$ (B) | 12 152.616(36) | 2676.0998(81) | 2197.0424(81) | 2.43(12) | *b* |
| $HNO_3$-$D_2O$ (A) | 11 990.170(41) | 2496.1501(75) | 2073.9628(75) | 2.03(11) | *b* |
| $HNO_3$-$D_2O$ (B) | 11 989.422(36) | 2496.1441(75) | 2073.9603(75) | 1.80(22) | *b* |
| $DNO_3$-$D_2O$ (A) | 11 831.839(51) | 2485.308(11) | 2061.706(11) | 2.10(11) | *b* |
| $DNO_3$-$D_2O$ (B) | 11 831.057(34) | 2485.3004(73) | 2061.7046(73) | 1.75(13) | *b* |
| $HNO_3$-DOH[c] | 12 066.005(34) | 2629.1699(10) | 2162.9632(10) | 2.420(41) | *b* |
| $DNO_3$-DOH[c] | 11 893.5(47) | 2616.400(13) | 2149.075(13) | 2.04(24) | *b* |

[a] Uncertainties are 1 standard error in the fit. [b] Fixed at the value for the A state of $HNO_3-H_2O$. [c] Corresponds to the isomer with the deuterium in the plane of the molecule.

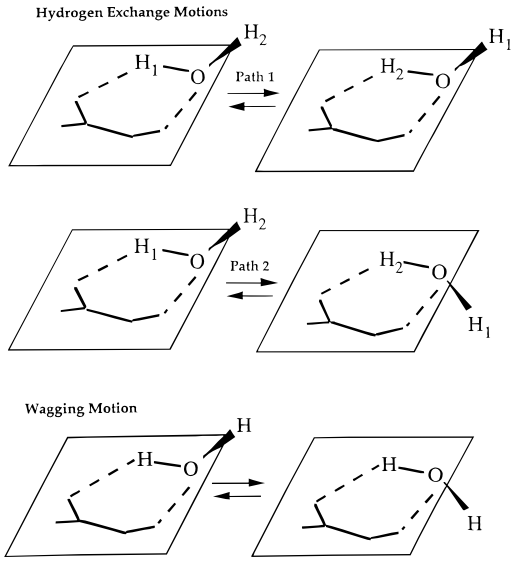


**Figure 2.** Several possible tunneling motions associated with the water subunit of $HNO_3-H_2O$. The *a* and *b* inertial axes of the complex lie very nearly in the molecular plane.

requiring the c-type transitions to *cross* the tunneling doublet. However, the hydrogen exchange motion cannot fully account for the experimental findings in this regard since the c-type transitions are absent *even for the DOH* species, in which the hydrogen interchange is quenched.

Figure 2 illustrates several plausible tunneling motions for the complex, given its geometry as predicted by theory[9] and deduced from experiment in the next section. The first two represent hydrogen exchange along two possible paths, labeled 1 and 2. Path 1 corresponds to the rotation of the $H_2O$ around its $C_{2v}$ axis, while path 2 corresponds to rotation of $H_2O$ around an axis perpendicular to its molecular plane. The latter path differs from the former in that it not only exchanges the two hydrogen atoms but also moves the out-of-plane H atom from one side of the heavy atom plane to the other. The third motion is simply a wag of the out-of-plane hydrogen above and below the plane of the complex.

A moment's inspection reveals that the in-plane dipole moment components, $\mu_a$ and $\mu_b$, both remain unchanged by any of the motions shown in Figure 2. $\mu_c$, on the other hand, which is perpendicular to the plane, is inverted by both the wag and the "path 2" hydrogen exchange. Thus, the lack of rigid rotor c-type transitions in the $H_2O$ and $D_2O$ complexes *could* be interpreted in terms of either the path 2 exchange *or* a wagging motion, *or both*. However, in the DOH complex, there *is* no exchange, and thus their absence is most plausibly interpreted as arising from motion along the wagging coordinate. Furthermore, we note that if such a motion were to occur in the DOH complex, there is no reason for it to cease in the $H_2O$ and $D_2O$ species. Indeed, wagging should be facile as it involves rotation about an O−H bond but not rupture of a hydrogen bond. Thus, in the $H_2O$ and $D_2O$ complexes we can presume that (unless $\mu_c$ were identically zero) a large amplitude wagging motion and perhaps additionally a path 2 hydrogen exchange are responsible for the absence of rigid rotor c-type transitions in the observed spectra.

The question as to whether $\mu_c = 0$ or the c-type transitions are displaced by a tunneling frequency associated with the wag cannot be definitively answered with the available data. It is pertinent to note, however, that the two possibilities arise as limiting cases of the same type of motion. If the zero point energy associated with the wag is large compared with the barrier height, then the complex is *effectively* planar and $\mu_c$, on average, is zero. On the other hand, if the zero point energy lies significantly below the barrier, the c-type transitions cross the associated tunneling doublet and are displaced from their rigid rotor positions by the tunneling frequency. The two scenarios smoothly correlate with one another, as the upper half of the tunneling doublet in the high-barrier case becomes the

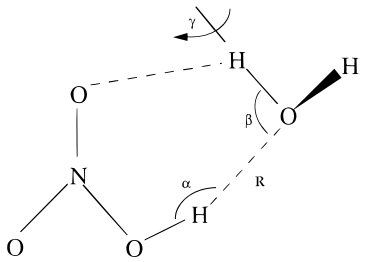


**Figure 3.** Intermolecular coordinates used to describe the structure of $HNO_3-H_2O$. Except for the free hydrogen of the water, the complex is assumed to be planar. See text for discussion.

first excited vibrational state of an effectively planar complex in the low-barrier situation.

Although the experimental data do not favor one description over the other, theory provides some useful insight. Tao et al.[9] report a barrier height of 83 $cm^{-1}$ at the planar configuration. Moreover, the vibrational frequency associated with the wag is 166 $cm^{-1}$.[27] Thus, it appears that the zero point energy is nearly coincident with the top of the barrier, and the system in fact lies *between* the two limiting cases described above. Clearly, however, with the zero point energy close to the barrier height, the proton will not be confined on either side of the molecular plane, and thus a delocalized picture in which $\langle \mu_c \rangle = 0$ on the time scale of rotations is probably the most realistic viewpoint. We note, also, that the 166 $cm^{-1}$ wagging frequency is consistent with the observation of only a single state for the HDO species and only two states for the $H_2O$ and $D_2O$ complexes. Indeed, rather than observing a closely spaced pair of "tunneling states" associated with the wag, only the "ground vibrational state" is observed at the nominally 2 K temperature of the supersonic jet.

Thus, to summarize, the observation of *two* states of the $H_2O$ and $D_2O$ complexes but only *one* state for the DOH species provides definitive evidence for an interchange motion involving the water hydrogens in the system. The available data, however, do not distinguish between the path 1 and path 2 motions in Figure 2. In addition, large-amplitude motion along the wagging coordinate is inferred from the apparent absence of rigid rotor c-type transitions in the DOH species, and an appeal to theory favors a picture involving a delocalized structure with $\langle \mu_c \rangle = 0$ on the time scale of rotations.

**Structure Determination.** Preliminary analysis of the measured rotational constants indicates a structure which is in rough agreement with the ab initio calculations of Tao et al.[9] The geometry is illustrated in Figure 2 and is shown in more detail in Figure 3. The system forms a planar, six-membered ring with a near-linear hydrogen bond between the $HNO_3$ proton and the oxygen of the water. The non-hydrogen bonded proton of the water lies above the molecular plane. Note that the angle $\gamma$, which describes the out-of-plane orientation nonbonded OH, is retained in the analysis and that this is not inconsistent with a vanishing value of $\langle \mu_c \rangle$ discussed above. In particular, while $\langle \sin \gamma \rangle$ may equal zero, the moments of inertia depend on $\langle \sin^2 \gamma \rangle$, whose value may differ from zero due to large-amplitude motion of the water subunit.

Initially, the rotational constants of the parent species ($HNO_3-H_2O$) indicated a hydrogen bond length of approximately 1.7 Å. This is in good agreement with the theoretical results, and indeed, as noted above, the basic geometry was readily confirmed by location of transitions due to other isotopic derivatives of the complex. Moreover, the inertial defect for state A of $HNO_3-H_2O$ is $-0.3799$ amu $Å^2$, a value which is somewhat *smaller* than the $-1.09$ amu $Å^2$ value calculated from the theoretical structure.[9] Thus, the data are also consistent with a planar complex having a single out-of-plane proton. Indeed, if the observed inertial defect were interpreted as arising entirely from the nonbonded hydrogen, the results indicate that the O−H bond lies about 27° out of the molecular plane.

The complex is sufficiently large that even the observation of eight isotopic derivatives does not permit the precise location of every atom in the complex. Nonetheless, information about the important intermolecular structural parameters can be obtained if, as is common for weakly bound complexes, the internal coordinates of the monomer units are fixed at their free-monomer values. That such a constraint is reasonably appropriate is supported by the 1.7 Å bond distance, which indicates a strongly hydrogen bonded system (rather than one in which the acidic proton has transferred to create $H_3O^+NO_3^-$). It should be noted, however, that the theoretical work on this system indicates that monomers *do* undergo finite distortions upon complexation.[9] However, the changes are small (e.g., typically less than a few hundredths of an angstrom in the bond lengths), and their effects can be incorporated into the model-dependent uncertainties in the quoted structural parameters, as described in more detail later on.

With the monomer geometries constrained, the structure of $HNO_3-H_2O$ can be specified in terms of the four intermolecular coordinates $R$, $\alpha$, $\beta$, and $\gamma$, shown in Figure 3. $R$ is the length of the hydrogen bond formed between the OH unit of $HNO_3$ and the oxygen of the $H_2O$. The angles formed between this hydrogen bond and the OH bonds of the $HNO_3$ and $H_2O$ are denoted as $\alpha$ and $\beta$, respectively. As noted previously, the acute angle between the out-of-plane OH bond and the heavy atom plane is $\gamma$. In principle, a puckering of the six-membered ring is also possible, but on the basis of the small inertial defect and on the previous ab initio results, a planar structure is assumed.

Using the known monomer structures of $HNO_3$[28,29] and $H_2O$,[30] a least squares fit of the ground (state A) rotational constants of the complex was performed to obtain the four parameters, $R$, $\alpha$, $\beta$, and $\gamma$. The results are given in the second column of the top portion of Table 5, listed under "undistorted monomers". The overall quality of the fit is indicated by the residuals in the rotational constants, which are also listed. It is readily seen that while most of the rotational constants are reproduced to within 5 MHz, seven of the calculated residuals lie in a range between 5 and 65 MHz, the most egregious values corresponding to the $A$ rotational constants of the deuterated water species. While this may at first seem somewhat disappointing, it is perhaps not entirely surprising for a system of this size and dynamic complexity. Indeed, the $A$ rotational constants are most sensitive to the angles $\beta$ and $\gamma$, which are the coordinates along which the large-amplitude motions of the water unit take place.

The standard errors in the structural parameters determined from the least squares fit to rotational constants are small and do not provide realistic estimates of the true uncertainties in the derived structure. Rather, the uncertainties are primarily model-related, arising both from the particular choice of the $HNO_3$ and $H_2O$ monomer geometries and from the large-amplitude motions which occur within the complex. These effects are discussed below.

The most significant perturbations of monomer structures reported by Tao et al.[9] involve changes in bond lengths and bond angles of several hundredths of an angstrom and 1−2°, respectively. To assess the effects of these changes on the fitted structure of the complex, the least squares fit was repeated with the calculated monomer distortions imposed on their experi-

**TABLE 5: Results of the Structure Fit for $HNO_3-H_2O$**

| Fitted Structural Parameters | | | | |
|---|---|---|---|---|
| param | undistorted monomers | fully distorted monomers | preferred structure | theoretical structure[a] |
| $R$ (Å) | 1.746 | 1.812 | 1.779(33) | 1.707 |
| $\alpha$ (deg) | 178.6 | 170.4 | 174.5(41) | 176.4 |
| $\beta$ (deg) | 90.4 | 93.4 | 92(8) | 101.3 |
| $\gamma$ (deg) | 29.9 | 30.3 | 30(10) | 49.9 |
| $R_{sec}$[b] (Å) | 2.32 | 2.27 | 2.30 | 2.49 |
| $\theta$(O···HO)[c] (deg) | 119.6 | 118.9 | 119.3 | 108 |

| Residuals of the Fitted Rotational Constants[d] | | | |
|---|---|---|---|
| | $A$ residual (MHz) | $B$ residual (MHz) | $C$ residual (MHz) |
| $HNO_3-H_2O$ | 0.73 | −0.80 | −0.75 |
| $HNO_3-H_2{}^{18}O$ | 0.31 | 0.66 | 0.26 |
| $H^{15}NO_3-H_2O$ | −3.4 | −0.53 | −0.50 |
| $DNO_3-H_2O$ | −4.7 | −3.9 | −2.9 |
| $HNO_3-D_2O$ | −60.0 | 10.3 | 6.9 |
| $DNO_3-D_2O$ | −65.4 | 7.4 | 4.6 |
| $HNO_3$−DOH | −35.0 | 0.46 | −0.37 |
| $DNO_3$−DOH | −53.7 | −2.5 | −2.7 |

[a] Reference 9. [b] Length of the secondary hydrogen bond between the water proton and the $HNO_3$ oxygen calculated from the fitted structure. [c] Angle between the secondary hydrogen bond and the in-plane OH bond of water calculated from the fitted structure. [d] Values obtained from a fit using undistorted monomer geometries.

mental geometries. The new values of the fitted parameters are given in the third column of Table 5, listed under "fully distorted monomers". In considering these results, it is perhaps worth noting that while the ab initio binding energy of the complex[9] has been corrected for basis set superposition error, the calculated geometries have not. The counterpoise correction may increase the intermolecular bond distance predicted by ab initio theory which in turn may reduce the predicted monomer distortions. Thus, the calculated monomer distortions probably represent upper limits to the true changes.[27] The best values of $R$, $\alpha$, $\beta$, and $\gamma$, therefore, are likely to lie between those resulting from the two fits.

The effects of large-amplitude motion are not as simple to assess. In the ideal situation, all rotational constants would be exactly reproduced by the fitted structure of the complex, but as large-amplitude motions become important, this no longer occurs. Thus, while the differences between the observed and calculated rotational constants *are not statistical*, the root mean squared (rms) residuals in their fitted values provide a rough indicator of the degree to which a rigid rotor model fails when forced upon this highly nonrigid system. In effect, we can crudely gauge the degree of structural imprecision due to large amplitude motions by calculating the changes in geometrical parameters necessary to account for typical residuals in the structure fit. This is roughly equivalent to determining a range of structures compatible with the full set of isotopic data.

Some numbers serve to illustrate. For the $B$ and $C$ rotational constants, which are most sensitive to $R$ and $\alpha$, the rms residuals calculated from Table 5 are 4.8 and 3.3 MHz, respectively. With these values, simple calculation shows that the "typical" residuals in $B$ and $C$ correspond to roughly a $\pm$0.005 Å spread in $R$ and a $\pm$0.3° spread in $\alpha$. Similarly, the $A$ rotational constants are most sensitive to $\beta$ and $\gamma$, and changes in the $A$ rotational constant by the rms residual of 39 MHz may be obtained by varying the values of $\beta$ of $\gamma$ by approximately 8 and 10°, respectively.

The fourth column of Table 5 lists the "preferred" intermolecular structural parameters of the complex. The values are taken as the averages of those obtained from fits using the undistorted and fully distorted monomer geometries (columns 2 and 3). For $R$ and $\alpha$, the uncertainties are dominated by the spread between the two columns, and the quoted values are chosen to encompass the two limiting cases. For $\beta$ and $\gamma$, the monomer distortions have little effect on the fitted parameters, and the 8 and 10° uncertainties derived above are used. The last column of the table lists the ab initio structural parameters of Tao et al.

**Nuclear Quadrupole Coupling.** To the extent that the $HNO_3$ is unperturbed upon complexation, the observed quadrupole coupling constants contain information about its angular orientation within the complex. In view of the ab initio results,[9] however, it seems likely that the $HNO_3$ *does* experience significant changes when bound to water. Nevertheless, it is of interest to check whether the measured quadrupole coupling constants of the complex are at least approximately compatible with the geometry reported above.

Using the geometrical parameters of $HNO_3-H_2O$ given in Table 5 and the known structure of the $HNO_3$ monomer,[28] the N−O single bond of $HNO_3$ lies at an angle of 55.9° relative to the $a$-axis of the complex. Moreover, Albinus et al.[31] have determined the orientation of the principal axis system, ($x$,$y$,$z$), for the quadrupole coupling tensor in free nitric acid. With their choice of axis labeling, the $x$-axis forms an angle of 16.6° with the $a$-axis of $HNO_3$, placing it at 1.1° with respect to the N−O single bond, rotated away from the hydrogen. Thus, the $x$-axis of free nitric acid lies at an angle of $\phi$ = 57.0° with respect to the $a$-axis of $HNO_3-H_2O$.

Albinus et al. have also reported the in-plane eigenvalues of the quadrupole coupling tensor of free nitric acid, $eQq_{xx}$ and $eQq_{yy}$, to be +1.103(19) and −1.033(21) MHz, respectively.[31] Thus, using the value of $\phi$ = 57.0° given above, a transformation to the inertial axis system of the complex gives values of $eQq_{aa}$ and ($eQq_{bb}$ − $eQq_{cc}$) equal to −0.399 and +0.539 MHz, respectively. Comparison of these results with the experimental values given in Table 3 at first suggests that the agreemet is rather poor. However, it is important to note that the trigonometric functions which enter into the tensor transformation equations are extraordinarily sensitive to $\phi$. Indeed, $eQq_{aa}$ can be brought into exact agreement with the observed value by changing $\phi$ to 59°, and the observed value of ($eQq_{bb}$ − $eQq_{cc}$) is similarly consistent with a rotation angle of 51°. Further, while the uncertainty in $\phi$ is difficult to estimate, a few degrees

does not seem unreasonable, given the level to which the structure of the complex is defined. Thus, we conclude that the observed $^{14}N$ hyperfine parameters are in acceptable agreement with the reported geometry. That different angles are necessary to reproduce the observed values of $eQq_{aa}$ and $(eQq_{bb} - eQq_{cc})$ may be indicative of slight electronic rearrangement within the $HNO_3$ moiety, but given the limitations inherent in the calculations, further analysis seems unwarranted.

## Discussion

The experimentally determined structure of $HNO_3-H_2O$ is in reasonably good agreement with the ab initio calculations of Tao et al.[9] and indicates that a strong hydrogen bonding interaction takes place between the two subunits of the complex. The primary hydrogen bond, identified by its near-linear geometry and short bond length, occurs between the acidic proton of $HNO_3$ and the oxygen of $H_2O$. Although a second hydrogen bond appears to exist between the in-plane proton of $H_2O$ and one of the $HNO_3$ oxygens, this bond does not meet the usual requirements of a "good" hydrogen bond because it is long (2.3 Å) and considerably bent (∼120°). Nevertheless, theoretical calculations indicate that this secondary interaction does offer some additional stability to the system.[9]

The two hydrogens on the water subunit of the complex are inequivalent, and thus, in principle, two isomers of the DOH species should be possible. As noted above, however, only a single form was observed for both $HNO_3-DOH$ and $DNO_3-DOH$, corresponding to an arrangement with deuterium in the plane of the complex, participating in a secondary hydrogen bond. This type of preference for placing deuterium in a hydrogen bond has been observed in a number of cases[32] and presumably arises from the reduced zero point energy associated with the heavier isotope. It is interesting to observe that such a zero point effect can play a significant role here as well, even through the secondary hydrogen bond. This supports the assertion by Tao et al.[9] that this secondary interaction provides additional stabilization to the complex.

While bulk phase reaction between $HNO_3$ and $H_2O$ gives rise to ionization, previous theoretical and experimental studies have concluded that the formation of the isolated 1:1 complex does not.[9,14,15b] The present results are in agreement with this conclusion. Certainly, the analysis of the internal dynamics is consistent with an independent $H_2O$ unit in the complex, and the isotopic shifts in the rotational constants support the hydrogen bonded structure. Also, while the uncertainties are somewhat large, the observed quadrupole coupling constants are roughly consistent with those calculated by simple projection of the coupling tensor onto the inertial axes of the complex. In addition, while a 1.78 Å hydrogen bond distance is somewhat short compared, for example, with the 1.931 and 1.987 Å distances in $H_2O-HCl$[33] and $H_2O-HBr$,[34] respectively, it is fairly similar to the 1.736 Å bond length in $H_2O-HF$.[35] Yet even in $H_2O-HF$, the $H_3O^+-F^-$ valence bond structure makes only a small contribution to the description of the complex.[36] Interestingly, previous experimental studies have suggested that gas phase $(HNO_3)(H_2O)_y$ clusters form solvated ion pairs, even at the small cluster level, but that the onset does not occur until the $HNO_3$ is hydrated with five water molecules.[37] In the crystal, however, even the monohydrate is ionic.[11]

Finally, in the context of previous work on cluster−induced modification of photolytic behavior,[7,8] and in light of the above-noted strength of the $HNO_3-H_2O$ interaction, it is interesting to comment on the possibility that clustering with water could affect the photochemistry of $HNO_3$. Interestingly, UV photolysis of nitric acid in cryogenic $N_2$ matrices has revealed significant changes in spectroscopic and photochemical behavior resulting from a specific $N_2-HNO_3$ interaction.[38] While the $N_2-HNO_3$ interaction energy is probably not well-known, it seems certain to be less than that of $H_2O-HNO_3$. Thus, these results suggest that further studies on the photochemistry of $HNO_3-H_2O$ may be an interesting avenue of exploration.

## Conclusion

The microwave spectrum and structure of the $HNO_3-H_2O$ complex have been determined via pulsed-nozzle Fourier transform microwave spectroscopy. The following conclusions may be drawn:

1. The complex is a cyclic, doubly hydrogen bonded system with a short (1.78 Å), near-linear hydrogen bond formed between the acidic proton of $HNO_3$ and the oxygen of $H_2O$. A second, presumably weaker interaction between one of the water protons and a nitric acid oxygen completes the ring. The complex is planar except for the non-hydrogen bonded proton of the water.

2. The structure obtained is in good agreement with ab initio calculations by Tao et al.[9] These calculations place the binding energy of the complex at 9.5 kcal/mol, a number which is particularly critical in terms of assessing the possible atmospheric importance of this system. We observe that, in the DOH containing species, only the isomers with the deuterium in the hydrogen bond are formed with any significant population in the jet. This provides experimental evidence in support of the assertion by Tao et al. that a secondary intermolecular O···H interaction exists and contributes to the overall binding energy of the system.

3. The water subunit of the system undergoes complex internal dynamics. A proton interchange motion in the $H_2O$ and $D_2O$ containing species is unambiguously established by an observed spectral doubling which disappears in the DOH complexes. A second type of large-amplitude motion is inferred from the absence of rigid rotor c-type transitions, even in the DOH species (where the proton interchange is quenched). This latter motion is interpreted in terms of large-amplitude wagging of the free hydrogen of the water.

**Acknowledgment.** This work was supported by the National Science Foundation (Grant No. ATM 9322809) and the Louise T. Dosdall Foundation. We are also grateful to Professor Bill Klemperer and Dr. John Crowley for providing preprints of refs 9 and 10, respectively, to Professors Fu-Ming Tao and Veronica Vaida for several enlightening discussions, and to an anonymous reviewer for pointing us to ref 31.

**Supporting Information Available:** Tabulations of spectral data including individual hyperfine frequencies (6 pages). Ordering information is given on any current masthead page.

## References and Notes

(1) Finlayson-Pitts, B. J.; Pitts, J. N., Jr. *Atmospheric Chemistry: Fundamentals and Experimental Techniques*; John Wiley and Sons: New York, 1986.

(2) Langford, A. O.; Fehsenfeld, F. C.; Zachariassen, J.; Schimel, D. S. *Global Biogeochem. Cycles* **1992**, *6*, 459.

(3) Crutzen, P. J.; Arnold, F. *Nature* **1986**, *324*, 651.

(4) Toon, O. B.; Hamill, P.; Turco, R. P.; Pinto, J. *Geophys. Res. Lett.* **1986**, *13*, 1284.

(5) Solomon, S. *Rev. Geophys.* **1988**, *26*, 131.

(6) Wennberg, P. O.; Cohen, R. C.; Stimpfle, R. M.; Koplow, J. P.; Anderson, J. G.; Salawitch, R. J.; Fahey, D. W.; Woodbridge, E. L.; Kleim, E. R.; Gao, R. S.; Webster, C. R.; May, R. D.; Toohey, D. W.; Avollone,

L. M.; Proffitt, M. H.; Lowenstein, M.; Podolske, J. R.; Chan, K. R.; Wofsy, S. C. *Science* **1994**, *266*, 398.

(7) (a) Frost, G. J.; Vaida, V. *J. Geophys. Res.* **1995**, *100*, 18803. (b) Vaida, V.; Frost, G. J.; Brown, L. A.; Naaman, R.; Hurwitz, Y. *Ber Bunsen-Ges. Phys. Chem.* **1995**, *99*, 371.

(8) Brown, L.; Vaida, V. *J. Phys. Chem.* **1996**, *100*, 7849.

(9) Tao, F.-M.; Higgins, K.; Klemperer, W.; Nelson, D. D. *Geophys. Res. Lett.* **1996**, *23*, 1797.

(10) Carl, S. A.; Ingham, T.; Moortgat, G. K.; Crowley, J. N. Submitted for publication.

(11) Delaplane, R. G.; Taesler, I.; Olovsson, I. *Acta Crystallogr.* **1975**, *B31*, 1486.

(12) Taesler, I.; Delaplane, R. G.; Olovsson, I. *Acta Crystallogr.* **1975**, *B31*, 1489.

(13) (a) Ritzhaupt, G.; Devlin, J. P. *J. Phys. Chem.* **1991**, *95*, 90. (b) Thi Pham, M.; Herzog-Cance, M. H.; Potier, A.; Potier, J. *J. Raman Spectrosc.* **1981**, *11*, 96. (c) Herzog-Cance, M. H.; Potier, J.; Potier, A.; Dhamelincourt, P.; Sombret, B.; Wallart, F. *J. Raman Spectrosc.* **1978**, *7*, 303. (d) Roziere, J.; Potier, J. *J. Inorg. Nucl. Chem.* **1973**, *35*, 1179. (e) Savoie, R.; Giguere, P. A. *J. Chem. Phys.* **1964**, *41*, 2698.

(14) Koller, J.; Hadzi, D. *J. Mol. Struct.* **1991**, *247*, 225.

(15) (a) Barnes, A. J.; Lasson, E.; Nielsen, C. J. *J. Mol. Struct.* **1994**, *322*, 165. (b) Ritzhaupt, G.; Devlin, J. P. *J. Phys. Chem.* **1977**, *81*, 521.

(16) Balle, T. J.; Flygare, W. H. *Rev. Sci. Instrum.* **1981**, *52*, 33.

(17) (a) Phillips, J. A.; Canagaratna, M. Goodfriend, H.; Grushow, A.; Almlöf, J.; Leopold, K. R. *J. Am. Chem. Soc.* **1995**, *117*, 12549. (b) Phillips, J. A. Ph.D. Thesis, University of Minnesota, 1996.

(18) Phillips, J. A.; Canagaratna, M.; Goodfriend, H.; Leopold, K. R. *J. Phys. Chem.* **1995**, *99*, 501.

(19) (a) Legon, A. C.; Wallwork, A. L.; Rego, C. A. *J. Chem. Phys.* **1990**, *92*, 6397. (b) Lovas, F. J.; Suenram, R. D.; Fraser, G. T.; Gillies, C. W.; Zozom, J. *J. Chem. Phys.* **1988**, *88*, 722. (c) Gutowsky, H. S.; Chen, J.; Hajduk, P. J.; Keen, J. D.; Emilsson, T. *J. Am. Chem. Soc.* **1989**, *111*, 1901. (d) Emilsson, T.; Klots, T. D.; Ruoff, R. S.; Gutowsky, H. S. *J. Chem. Phys.* **1990**, *93*, 6971.

(20) Chilton, T. H. *Strong Water Nitric Acid: Sources, Methods of Manufacture, and Uses*; MIT Press: Cambridge, MA, 1968; p 166.

(21) The constancy of these splittings for the observed b-type transitions of a given isotopomer is to be expected since their magnitude is dominated by the difference in *A* rotational constants between the two tunneling states.

(22) For the cases of $HNO_3-H_2O$ and $HNO_3-H_2{}^{18}O$ there were groups of transitions that completed "closed loops" among relevant energy levels. These closed loops were also consistent with the A and B assignments that were based on intensity.

(23) (a) Townes, C. H.; Schawlow, A. L. *Microwave Spectroscopy*; Dover: New York, 1975. (b) Gordy, W.; Cook, R. L. *Microwave Molecular Spectra*; John Wiley and Sons: New York, 1984.

(24) Robinson, G. W.; Cornwell, C. D. *J. Chem. Phys.* **1953**, *21*, 1436.

(25) Watson, J. K. G. *J. Chem. Phys.* **1967**, *46*, 1935.

(26) While most of the residuals in these fits fell within two standard errors of the reported line centers, a very small number of the $HNO_3-H_2O$ and $HNO_3-H_2{}^{18}O$ line centers lie outside this range by a few kilohertz. It was noted that the addition of a $\delta_J$ term of approximately 0.3 kHz helped reduce these residuals. However, despite repeated attempts, it was not possible to obtain a fully converged value of $\delta_J$ because singular Hessian matrices were produced during the minimization process. Since the contribution from $\delta_J$ was only on the order of a few kilohertz, attempts to include it in the fit were not further pursued.

(27) Tao, F.-M. Private communication.

(28) Cox, A. P.; Riveros, J. M. *J. Chem. Phys.* **1965**, *42*, 3106.

(29) Millen, D. J.; Morton, J. R. *J. Chem. Soc.* **1960**, 1523.

(30) Cook, R. L.; DeLucia, F. C.; Helminger, P. *J. Mol. Spectrosc.* **1974**, *53*, 62.

(31) Albinus, L.; Spieckermann, J.; Sutter, D. H. *J. Mol. Spectrosc.* **1989**, *133*, 128.

(32) See, for example: Leung, H. O.; Marshall, M. D.; Suenram, R. D.; Lovas, F. J. *J. Chem. Phys.* **1989**, *90*, 700.

(33) Legon, A. C.; Willoughby, L. C. *Chem. Phys. Lett.* **1983**, *95*, 449.

(34) Legon, A. C.; Suckley, A. P. *Chem. Phys. Lett.* **1988**, *150*, 153.

(35) Bevan, J. W.; Kisiel, Z.; Legon, A. C.; Millen, D. J.; Rogers, S. C. *Proc. R. Soc. London* **1980**, *A372*, 441.

(36) Legon, A. C.; Millen, D. J. *Chem. Soc. Rev.* **1992**, *21*, 71.

(37) Kay, B. D.; Hermann, V. A. W.; Castleman, A. W. *Chem. Phys. Lett.* **1981**, *80*, 469.

(38) Chen, W. J.; Lo, W. J.; Cheng, B. M.; Lee, Y. P. *J. Chem. Phys.* **1992**, *97*, 7167.